Desalination and Water Treatment
www.deswater.com
doi: 10.5004/dwt.2020.26023

198 (2020) 407–421
September

Commercial waste wood in the removal of methylene blue from aqueous media

Aziz Ahmadi[a], Svetlana Ignatova[b], Mohammad Reza Ketabchi[c], Peter Clough[d], Salman Masoudi Soltani[b,*]

[a]*Department of Mechanical and Aerospace Engineering, Brunel University London, UB8 3PH London, UK, email: 1506341@alumni.brunel.ac.uk (A. Ahmadi)*
[b]*Department of Chemical Engineering, Brunel University London, UB8 3PH Uxbridge, UK, Tel. (+44)-(0)1895265884; emails: Salman.MasoudiSoltani@brunel.ac.uk (S. Masoudi Soltani), svetlana.ignatova@brunel.ac.uk (S. Ignatova)*
[c]*Department of Chemical and Environmental Engineering, Faculty of Engineering, University of Nottingham, Malaysia Campus, 43500 Semenyih, Selangor, Malaysia, email: mr.ketabchi@yahoo.com (M. Reza Ketabchi)*
[d]*Centre for Climate and Environmental Protection, Cranfield University, MK43 0AL Bedford, UK, email: P.T.Clough@cranfield.ac.uk (P. Clough)*

Received 9 September 2019; Accepted 24 April 2020

ABSTRACT

This study investigates the adsorption capacity and the kinetics of commercial waste wood in the UK, used as solid fuel, in the removal of methylene blue (MB) dye from aqueous media. The experiments were designed according to a fractional factorial design of experiment (DoE) framework, that is, Taguchi DoE, enabling us to reveal the possible inter-parameter interactions and also to pinpoint the optimum experimental envelopes via a statistically-systematic approach. The optimum removal efficiency (i.e. 96.7%) was achieved with a solution pH = 5, an adsorbent dosage = 4 g/L, an initial dye concentration = 0.015 g/L, and with a mixing speed of 30 rpm. The adsorption process was found to be exothermic. The adsorbent was saturated after approximately 60 min, corresponding to a maximum experimental adsorption capacity of 4.8 mg/$g_{adsorbent}$. The adsorption was best described by Freundlich isotherm. The maximum theoretical monolayer adsorption capacity was found to be 29.5 mg/$g_{adsorbent}$. The adsorption kinetics followed a pseudo-second-order model. The dimensionless factor, R_L, indicated that the adsorption process was favorable. The results indicate that the waste wood used in this study could be utilized as a low-cost and efficient adsorbent for MB removal. However, further studies investigating the leaching behavior of this waste wood are deemed to be of key importance before any large-scale application of this waste biomass stream.

Keywords: Adsorption; Waste wood; Methylene blue; Taguchi; Design of experiments

1. Introduction

Textile industries are well known for extreme water pollution and inadequate solid waste management. Studies have reported the presence of over 8,000 chemicals and about 1.6 million L of water per day in fabric production lines [1]. Wastewater streams generated in textile industries contain toxic synthetic dyes that must be removed/diluted prior to disposal into the environment. These dyes would leave adverse impacts on fragile ecosystems around the industries and have been associated with serious environmental problems [2]. Industrial dyes are typically classified based on their particle charge upon dissolution in aqueous solutions: anionic (direct, acidic, and reactive dyes), cationic (all basic dyes), and non-ionic (dispersed dyes) [3]. The intensity of colors associated with the basic dyes is very

* Corresponding author.

high, making them readily visible even in low concentrations. These dyes are typically carcinogenic, mutagenic, and/or teratogenic [4]. They can cause severe damage to the human body, which is the kidney, reproductive system, liver, brain, and the central nervous system [5]. Dye contamination is linked to many types of cancer developments in different organs including bladder, spleen, liver, and normal aberrations in model organisms and chromosomal deformities in mammalian cells. The typical dye concentration in textile wastewater processing effluent is between 10 to 200 mg/L [6].

Physicochemical, biochemical, bio-electrochemical, and thermo-chemical techniques have been suggested in removing contaminants from wastewater coming from textile industries [7]. The treatment has to be cost-effective. In order to do this, the utilization of solid waste materials, for example, biomass waste has been suggested. These could be good alternatives to traditional (and relatively costly) adsorbents. This is due to economic feasibility, simplicity of design, and often, high removal efficiencies [8]. During the past decade, there have been many reported on the use of organic adsorbents: almond shell, peanut husk, sesame hull, tea waste, date pits, date stones, jackfruit peel, pomelo skin, oil palm biodiesel solid residue, pistachio nutshell, pineapple peel, orange peel, coconut shell, apricot stones, palm date seed, wheat straw, rice straw, Foumanat tea, bamboo, sugarcane bagasse, swede rape straw, cocoa shell, pistachio hull, peach shell, sugar beet pulp, banana peel, peanut sticks wood, coconut coir, walnut shell, ginger waste, white rice husk ash, sour cherry stones, macauba seeds, pomegranate peel, barley straw, pecan nutshells, apricot stones, water hyacinth leaves, garlic peel, mustard husk, potato peels, grape stalk, mung bean husk, sunflower seed shells, soya stalks, orange peels and corncob [9]. More recently, scientists have grafted acrylamide and citric acid groups onto rice straws to remove dyes [10]. As a result, the adsorption capacity for methyl orange, methylene blue (MB), $Cr_2O_7^{2-}$ and Cu^{2+} in the mixed system increased by 210%, 133%, 196%, and 151%, respectively. Other researchers have developed sorbents containing cyclodextrins and have reached pollutant concentrations of <0.001–1 μg/L using cyclodextrin bead polymer [11]. On the other hand, only a few studies have focused on the optimization of the adsorption process itself.

Most of the literature is; however, centered on the adaptation of a linear individual parametric model by which the interaction among the experimental parameters and their significance could potentially be overlooked. In this study, we have employed a Robust (Taguchi) design of experiment (DoE) to reveal the presence of any possible inter-parameter interactions and also to systematically identify the significant variables affecting the efficiency of the adsorption. In our previous paper [12], we successfully studied the effects of pyrolysis conditions on the porous structure of mesoporous carbon derived from used cigarette filters using a full factorial DoE framework. However, the application of Taguchi DoE in adsorption experiments has been studied by only a few researchers as of today: an experimental optimization for Cu removal from aqueous solution using neem leaves adopted the Taguchi method [13]. The authors used Taguchi (L16) orthogonal array to optimize the experimental conditions.

In this study, we have used a commercially available waste wood as an adsorbent to remove MB from aqueous solutions. Waste wood comes from different sources such as demolition, wood processing and manufacturing, pallets, wooden packaging, and municipal wood waste and can pose environmental concerns and challenges upon its disposal, for example, landfilling. At the same time, releasing large amounts of industrial colored wastewater has created biological problems [14]. Such polluted wastewaters eventually end up in the marine environment. Every year, over 10^5 types of commercially-available dyes are being produced [15]. The dyes in water are highly visible and undesirable. Rapid growth in population and industrial productions would result in large amounts of highly polluted water resources carrying dyes and solid wastes. Their resistance to degradation, adsorption, light, water, and oxidizing agents demand more efficient removal methods. Various removal processes including adsorption, coagulation, oxidation, filtration, and ionizing radiation have been investigated. Adsorption, an effective method, has been long used in removing dyes from wastewater. However, it can be costly – depending on the adsorbent used. Waste wood, a commercial solid waste used as solid fuel, has been studied in this work for its adsorption capacity of MB. We have also investigated the adsorption kinetics and have revealed any interactions among the experimental parameters involved via a systematically-sound statistical approach.

2. Materials and methods

2.1. Preparation of the adsorbent

Waste wood pellets were supplied by Stobart Group, (UK) which were then ground and sieved (mesh #50). The supplied waste wood is typically used as fuel in power generation in the country. The particle size distribution of the waste wood powder was measured on a Zetasizer Nano series (Nano S) particle size analyzer. The porous area of the waste wood was measured on a nitrogen adsorption–desorption machine (TriStar 3000 V6.07). The total (micro + meso) and microporous surface areas were determined via Brunauer–Emmett–Teller (BET) and *t*-plot models, respectively. Pore size distribution was determined via the Barrett–Joyner–Halenda (BJH) method, applied to the adsorption branch of the nitrogen adsorption/desorption isotherm. The proximate analysis of waste wood was done on a thermogravimetric analyzer (TGA Q5000 V3.17 Build 265). The TGA was flushed with oxygen and/or nitrogen throughout the runs. The gas flow rates were individually controlled. A small amount of waste wood was transferred onto an alumina crucible and then inside the TGA before the test.

The surface functional groups of waste wood were detected on Fourier-transform infrared spectroscopy (FTIR) in the range of 600–4,000 cm^{-1} (Perkin Elmer, USA). The attenuated total reflection (ATR) method was used to directly analyze the powder samples without the need to mix the samples with KBr or any liquid paraffin. The ATR method involved pressing the sample against a high-refractive-index diamond prism and measuring the infrared spectrum using infrared light that was totally and internally reflected in the prism.

The surface morphology of the waste wood was studied on a scanning electron microscope (SEM Zeiss SUPRA 35 VP). An accelerating voltage of 10 kV in a highly-vacuumed environment was applied. Prior to any analysis, the samples were dried and were stored in a desiccator for 2 d. In the SEM experiments, a small amount of sample was placed on a small carbon tape and then placed on an aluminum platform.

2.2. Adsorbate

MB was purchased from Sigma-Aldrich (Germany) and was used as an adsorbate as received without any further purification.

2.3. Taguchi DoE and the equilibrium studies

Taguchi DoE was employed in order to optimize the experimental parameters and reveal any inter-parameter interactions among the experimental variables. The DoE framework was developed using Minitab 18 software. Taguchi uses a special design of orthogonal arrays to study the entire parametric space with a statistically-reduced number of experiments. It employs a standard orthogonal array comprising experimental variables each associated with a different level.

In our experiments, an orthogonal array was employed using four experimental parameters (i.e. solution pH, dye concentration (mg/L), adsorbent dosage (g/L) and mixing speed (rpm)), each with four levels and combinations in an equal number of occurrences to generate a balanced DoE. The layout of the orthogonal array (L16 (4^4)) comprises four operational variables, each studied at four levels corresponding to a total number of sixteen experiments.

Four aqueous MB stock solutions (i.e. 0.005, 0.01, 0.015, and 0.020 g/L) were prepared in 200 mL analytical flasks. 25 mL of each dye solution was transferred into a beaker for pH adjustment using NaOH (1 M) or HCl (1 M) solutions. The pH value was recorded using an ultrabasic pH meter. Different amounts of waste wood (i.e. 0.05, 0.1, 0.15, and 0.2 g) were prepared to a known weight (Denver M-220D digital scale). The dye solutions were transferred into 40 mL glass vials to mix with the adsorbent. Each vial was placed on a rotator for continuous mixing until the equilibrium was reached (i.e. 5 h). The solution was then centrifuged. The absorbance of the supernatant liquids was measured on a UV-1800 Shimadzu spectrophotometer (Japan) at a wavelength of 664 nm (i.e. the wavelength corresponding to the maximum absorbance observed). From the absorbance, the adsorption capacity and the dye percentage removal were calculated using Eqs. (1) and (2):

$$q_e\left(\text{mg/g}\right)=\frac{\left(C_0-C_e\right)V}{m} \tag{1}$$

$$\text{Removal}\left(\%\right)=\frac{C_0-C_e}{C_0}\times 100 \tag{2}$$

where q_e is the amount of MB adsorbed by the waste wood (mg/g), C_0 and C_e are the initial and final dye concentrations (mg/L), respectively; V is the volume of solution (L) and m is the adsorbent dosage (g) [8].

Each experiment was run in triplicates and the mean adsorbent capacity (q_e) and the percentage removal (%) were recorded (Table 1). Subsequently, the adsorbent capacity, q_e (mg/g), and the percentage removal (%) obtained from the formulae above were fed back into the Taguchi table on Minitab 18 for further analyses.

Table 1
Calculated adsorbent capacity, removal percentage and the corresponding signal-to-noise based on Taguchi L16 orthogonal array DoE (Mean 1 and Mean 2 are the S/N ratios for the two control factors)

pH	Adsorbent dosage (g/L)	Initial dye concentration (mg/L)	Round per Minute (RPM)	Adsorption capacity q_e (mg/g)	Removal (%)	Mean 1	Mean 2
3	2	5	25	2.347	93.88%	2.347	0.9388
3	4	10	30	2.422	96.89%	2.422	0.9689
3	6	15	35	2.423	96.90%	2.423	0.9690
3	8	20	40	2.413	96.50%	2.413	0.9650
5	2	10	35	4.827	96.53%	4.827	0.9653
5	4	5	40	1.200	96.00%	1.200	0.9600
5	6	20	25	3.224	96.71%	3.224	0.9671
5	8	15	30	1.813	96.72%	1.813	0.9672
7	2	15	40	7.233	96.47%	7.233	0.9647
7	4	20	35	4.829	96.57%	4.829	0.9657
7	6	5	30	0.798	95.25%	0.798	0.9525
7	8	10	25	1.207	96.53%	1.207	0.9653
9	2	20	30	9.622	96.20%	9.622	0.9620
9	4	15	25	3.634	96.88%	3.634	0.9688
9	6	10	40	1.601	95.95%	1.601	0.9595
9	8	5	35	0.593	94.49%	0.593	0.9449

3. Results and discussion

3.1. Characterization of the adsorbent

The adsorption isotherm (Fig. 1) is a type IV isotherm according to the International Union of Pure and Applied Chemistry classification, indicating the mesoporous nature of the adsorbent. This type of isotherm is consistent with a structure in which both open and blocked cylindrical mesopores can exist.

The BET surface area, BJH cumulative pore volume and the average pore diameter of the waste wood were calculated to be 0.58 m^2/g, 5.6 × 10^{-3} cm^3/g and 63.9 nm, respectively. Higher adsorption capacity is justified on the basis of the higher average pore diameter of the waste wood. As observed in similar studies, the adsorption was based on a monolayer chemical adsorption mechanism in the single pollutant system [10]. The dye particles are attached to the adsorbent's surface functional groups. These surface functional groups have been identified and described in the following sections.

The SEM images of the waste wood before and after adsorption of dye are shown in Fig. 2. It can be seen that before the adsorption, the surface of the waste wood is smooth (Fig. 2a), while after the adsorption of MB, the surface has become slightly coarser (Fig. 2b). This suggests the presence of interaction and compatibility between MB

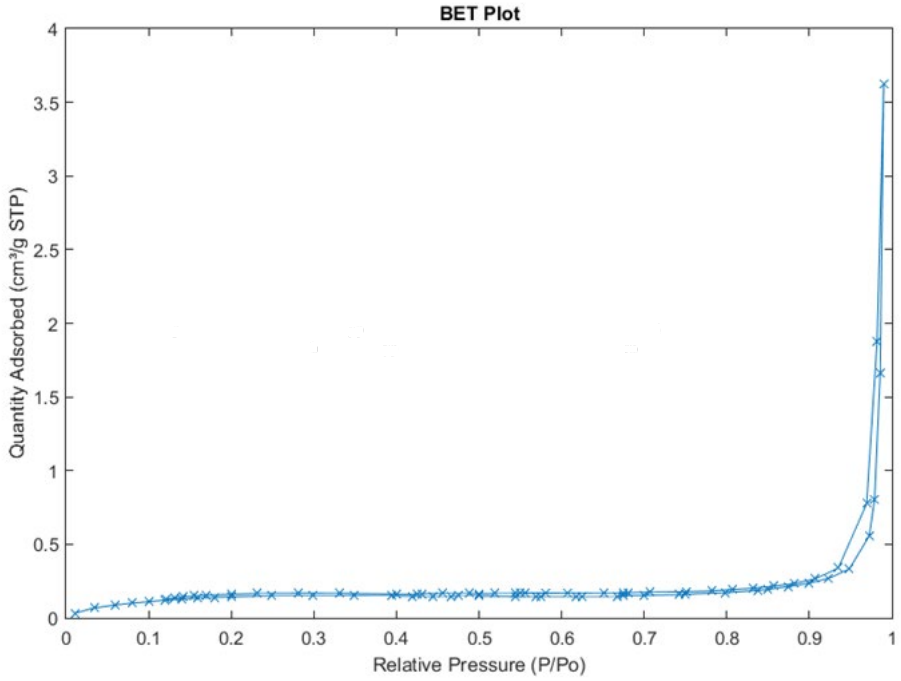

Fig. 1. BET surface area plot for the waste wood used in this study.

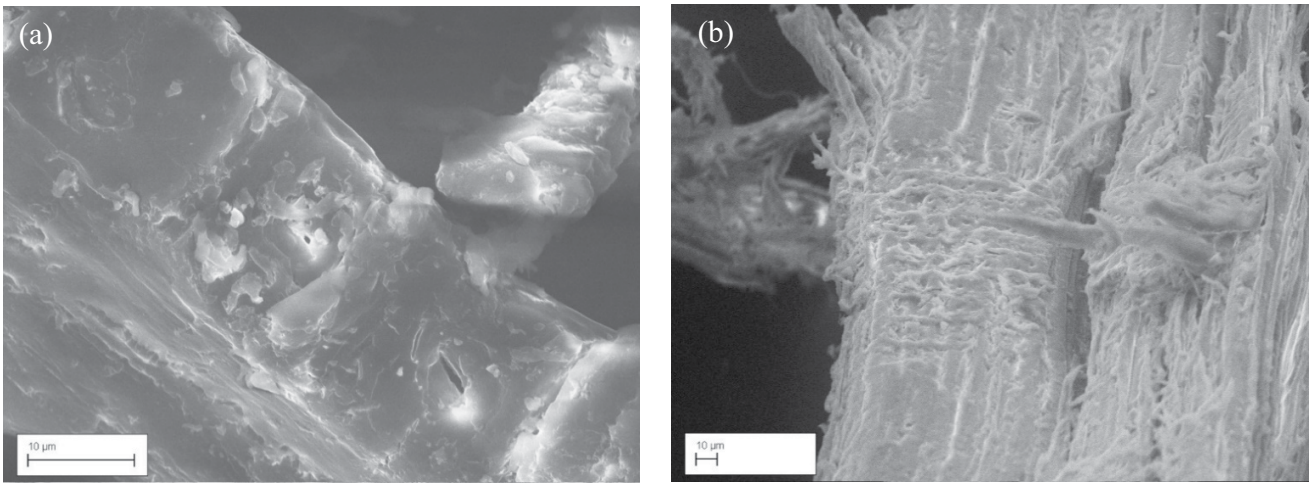

Fig. 2. SEM images of the adsorbent surface (a) before and (b) after MB adsorption.

molecules and the adsorbent surface, altering the surface morphology upon surface adsorption.

Proximate analysis was done to find out the carbon, moisture, volatile, and ash contents of the waste wood biomass as shown in the TGA graph in Fig. 3. The sample was heated in an inert nitrogen atmosphere from 323 to 383 k and was kept at this temperature for 20 min in order to eliminate the moisture content. Thereafter, the temperature was raised to 873 k and the temperature was maintained for 30 min. The weight loss percentage at this point was an indication of the volatile matter present in the waste wood. The temperature was then reduced to 872 k at which point the weight dropped from 20% to 2% indicating the ash content of the waste wood used in this work.

The adsorption capacity of the waste wood depends on the nature and the interaction of the functional groups accessible on the surface. These surface functional groups, detected by an FTIR, are shown in Fig. 4. The FTIR spectrum of the adsorbent shows broad bands at 3,326 cm^{-1} due to the OH stretch. The absorption band at 2,891 cm^{-1} is due to the contribution from C–H stretching. The stretching vibration at 1,595 cm^{-1} is attributable to the presence of C=C bonds. In addition, the infrared spectrum shows an absorption band at 1,506 cm^{-1}, indicating the presence of aromatic rings. The presence of Si–O linkage is confirmed by the peak at 1,025 cm^{-1}. After the adsorption process was complete, some functional groups were seen to have shifted from their initial positions. The adsorption band at 3,326 cm^{-1} shifted to 3,329 cm^{-1} due to the presence of the adsorbed MB molecules. The adsorption band at 2,891 cm^{-1} also shifted to 2,898 cm^{-1}. These shifts were due to the new hydrogen bonding (the hydroxyl groups). The big difference in the frequency band was observed just after the aromatic region where before the adsorption the stretching vibration occurred at 1,368 cm^{-1}. After MB adsorption, the stretch moved to 1,330 cm^{-1}.

3.2. Analysis of variance

In order to investigate the normal distribution of the data, as a mandatory prerequisite to allow for the analysis of variance (ANOVA) of the experimental data, the response values must pass the normality test. The normality test confirmed that the response data set was normal with a p-value of 0.438 (i.e. >0.05) – affirming that ANOVA for this data can now be safely performed.

3.2.1. Main effects plots

The main effects plots were produced on Minitab 18 and are shown in Fig. 5. The means for each value of a categorical variable is plotted against the experimental parameters. The plot shows that MB removal% is the highest at pH = 5. The optimum adsorbent dosage is 4 g/L. The graph also shows that MB removal% increases with an increase in the initial MB concentration up to an initial concentration of 0.015 g/L, corresponding to a removal efficiency of 96.7%. However, with a further increase in the initial MB concentration to 0.020 g/L, the removal efficiency drops. This could be mainly due to the saturation of the adsorption sites on the adsorbent.

The sharp increase in the removal% with an increase in the initial MB solution concentration can be due to the abundance of dye molecules in the solution which may come in contact with the surface functional groups of the adsorbent.

3.2.2. Interaction plot using ANOVA

On the main effect plots (Fig. 5), the effect of a single independent variable on a dependent variable is revealed. This, however, overlooks the potential interaction among the independent variables. The interaction plots were generated

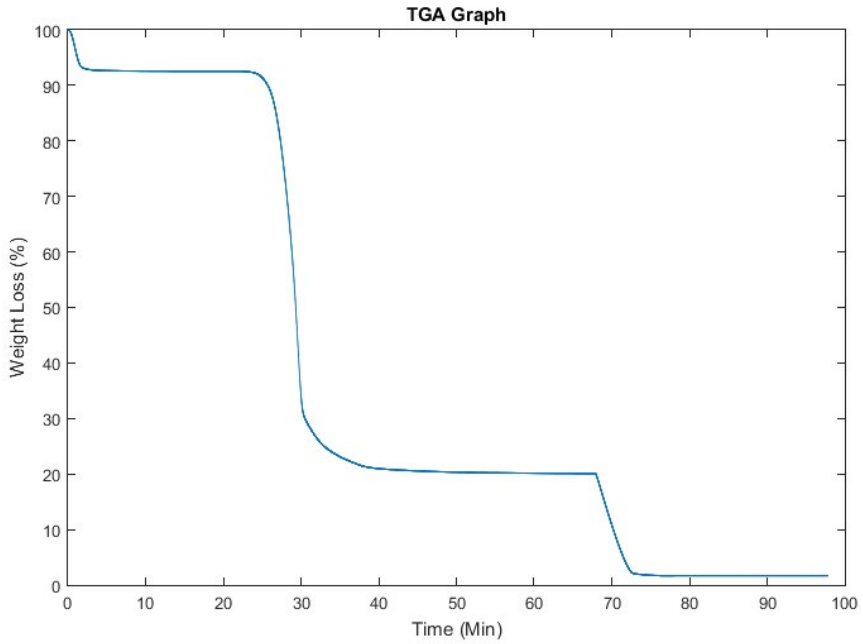

Fig. 3. TGA graph produced as a result of the proximate analysis of the waste wood.

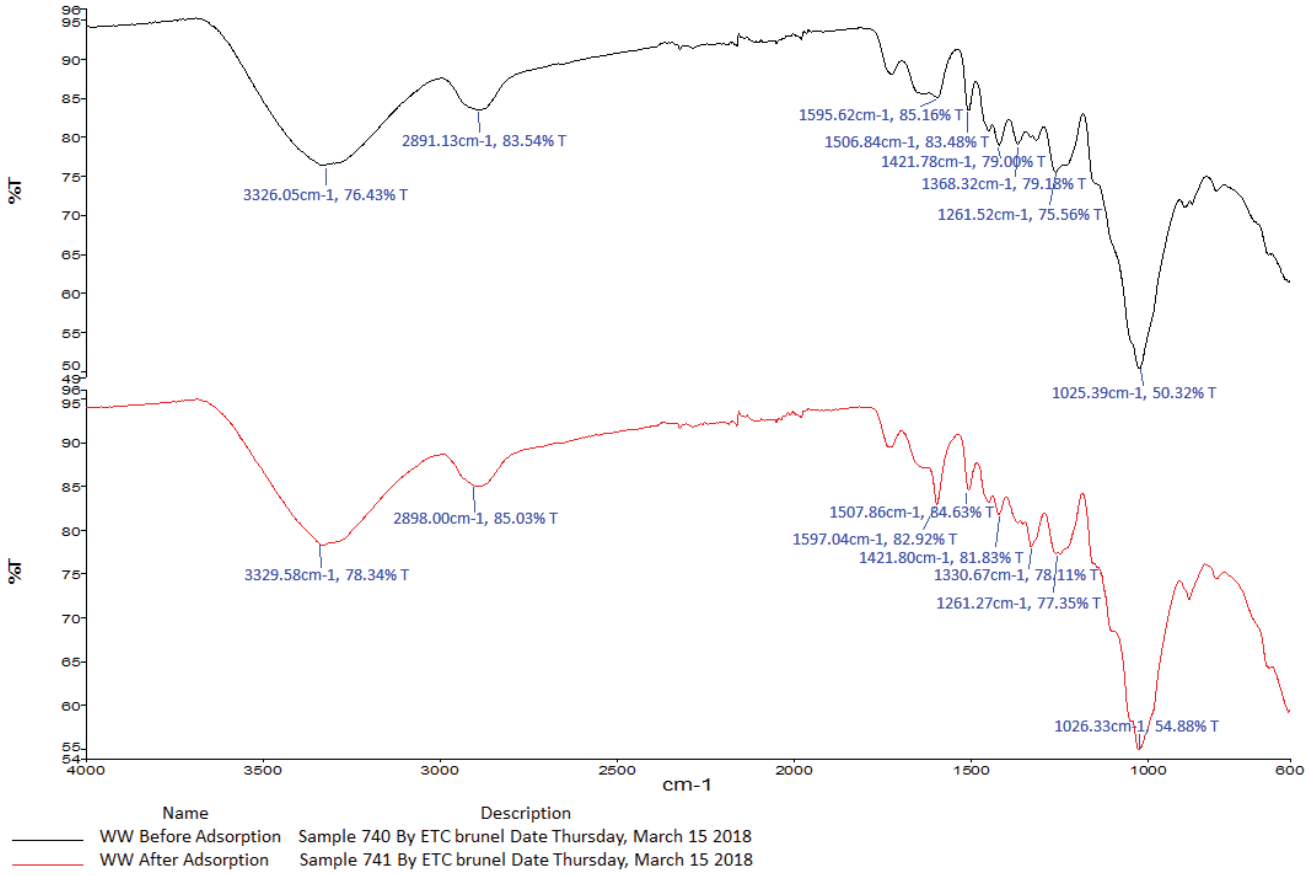

Fig. 4. FTIR spectrum for before (top graph) and after (bottom graph) MB adsorption.

Fig. 5. The main effects plots for MB removal%.

in Minitab 18 and are shown in Fig. 6. Fig. 6 illustrates the presence of strong interactions among the experimental parameters and their effects on MB removal efficiency.

From the interaction plots, the highest MB removal% is achieved with 4 g/L of adsorbent and an initial MB concentration of 0.015 g/L as indicated by the green line in Fig. 6. Also, a mixing speed of 30 rpm corresponds to the highest removal%.

3.2.3. Surface plot for removal%

A predictive response surface plot is constructed based on the principles of response surface methodology (RSM). It is a 3-dimensional graph with the predictor values on the x and y-axis and continuous surface representing the response values (i.e. the dependent variable). Fig. 7 illustrates how MB removal% varies as a function of the adsorbent dosage and the initial dye concentration.

The RSM plot clearly identifies the optimum conditions for maximum MB removal. The advantage of RSM is that it can reduce the number of experimental trials and evaluate the interactions between multiple parameters. The peaks on the plot correspond with the highest MB removal % for adsorbent dosages of 4 and 6 g/L and initial dye concentrations of 0.010 and 0.015 g/L. As expected, the lowest removal% is observed at the lowest level of adsorbent dosage (2 g/L) and an initial dye concentration of 0.005 g/L.

3.3. Effect of temperature on MB adsorption

The effect of temperature on the adsorption capacity and the removal efficiency is shown in Fig. 8. It is seen that both the adsorption capacity of the adsorbent and the removal % drop with an increase in the temperature.

Fig. 8 shows that the adsorption process is exothermic which can be due to a reduction in the adsorptive interactions between the dye molecules and the active sites on the adsorbent surface [16]. Adsorption reaction of MB onto pineapple leaf powder and clay were similarly found exothermic in nature [17,18]. This can also be due to the tendency of the MB molecules to escape from the surface of the solid phase into the solution with an increase in the temperature [19]. Therefore, the lower the temperature, the more facilitated the adsorption process becomes. Similar results have been reported in the literature for malachite green [8] and MB [20].

3.4. Effect of contact time on MB adsorption (equilibrium and kinetics studies)

Kinetics and equilibrium studies provide insights into the actual feasibility of a large-scale process [21]. It is observed that fast uptake of MB takes place during the initial stages of the adsorption process after which the adsorption rate gradually drops until it levels off where no more MB molecules can be removed from the solution (i.e. the equilibrium/saturation point). Fast adsorption can be an indication of sufficiently large specific surface areas, pore volumes, and appropriate porous structures of the adsorbent [22]. The fast adsorption of MB takes place within the first 5 min of the experiment, corresponding to a removal of about 94% at the end of this period (Fig. 9). After this phase, the adsorption rate significantly drops. The equilibrium is reached after approximately 60 min, corresponding to a maximum adsorption capacity of about 4.8 mg/g.

The higher initial adsorption rate is due to the availability of the surface groups. These sites are gradually taken up by MB molecules, leading to a reduction in the available sites for the residual MB molecules in the solution. The adsorption

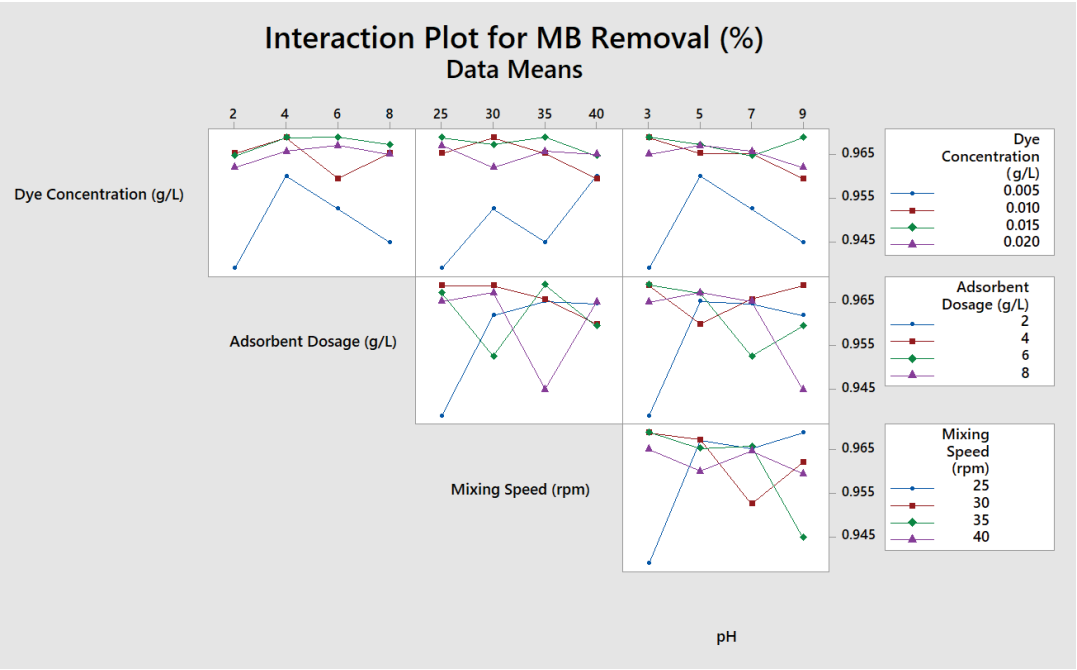

Fig. 6. Interaction plot for the removal%.

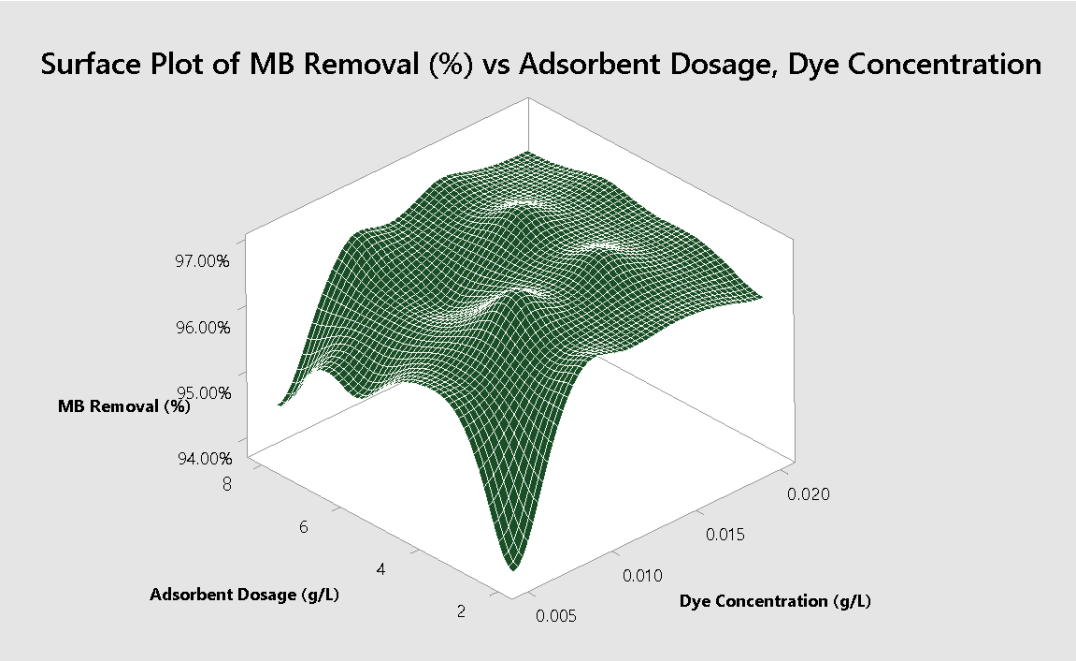

Fig. 7. Surface plot – removal % as a function of adsorbent dosage and initial MB concentration.

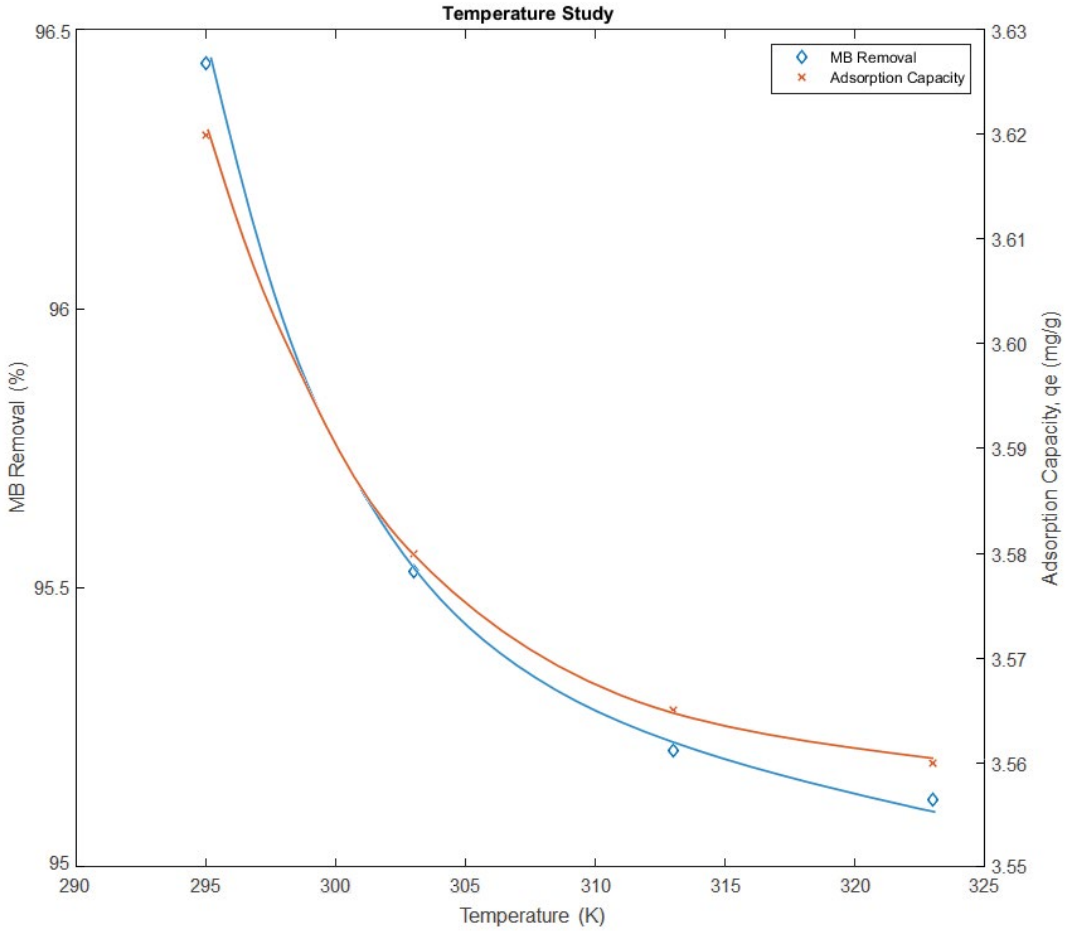

Fig. 8. Effect of temperature on the adsorption capacity and MB removal efficiency.

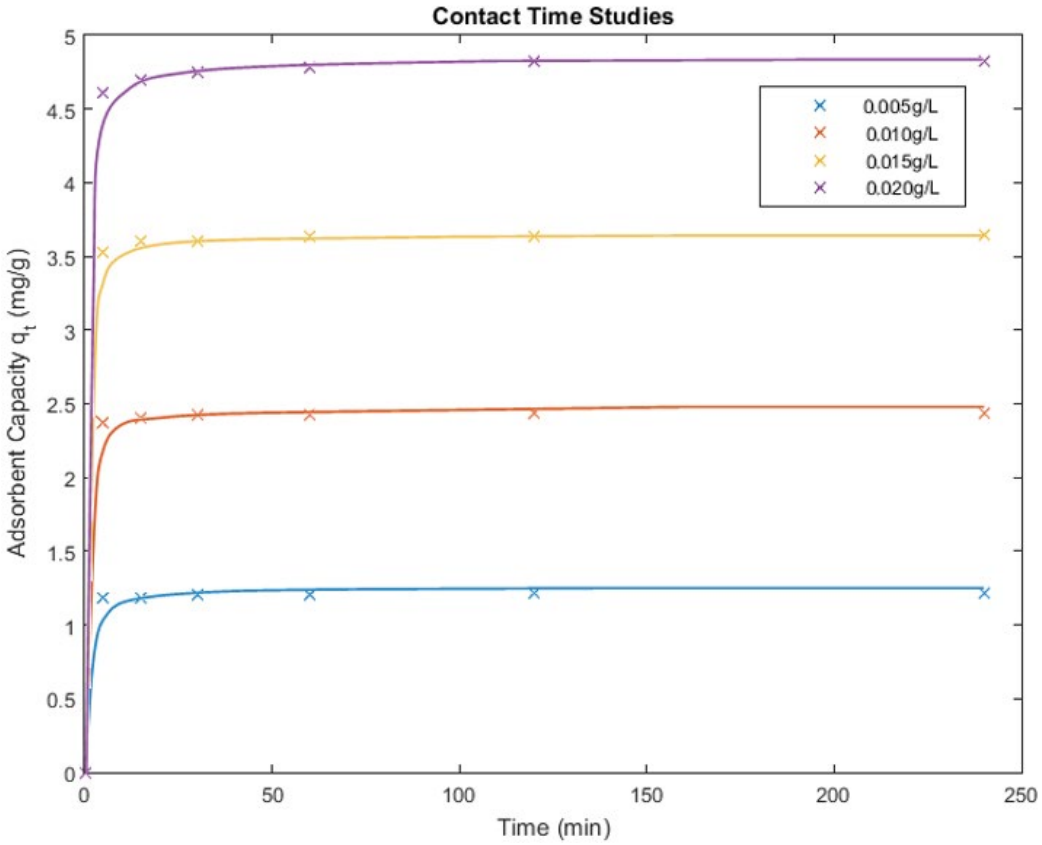

Fig. 9. Effect of contact time on MB adsorption at 295 K.

process can, therefore, be divided into two phases: an initial high adsorption rate phase within the first 5 min (rapid adsorption of dye molecules on the adsorbent surface), followed by a second phase associated with a very slow adsorption rate, eventually leading to the saturation (equilibrium) state. This is due to the fact that the remaining surface groups are difficult to be occupied as a result of the repulsion between the solute molecules already adsorbed onto the adsorbent's surface and the ones in the bulk of the solution [23]. Consequently, it is also observed that the higher the MB concentration, the longer it takes for the equilibrium state to be reached.

3.5. Adsorption isotherms

When the adsorbent and adsorbate are brought to and remain in contact long enough, an equilibrium state is eventually reached between the amount of adsorbate adsorbed and the amount of adsorbate present in the solution. The equilibrium relationship is described by the adsorption isotherms. Adsorption isotherms provide information on the nature of the interaction between the adsorbent and the adsorbate and reveal the adsorption capacity of a particular adsorbent for a specific adsorbent. Among the many available isotherm models in the literature, Langmuir and Freundlich's models are the most widely used to describe adsorption isotherms [24] and have been, therefore, employed to study the adsorption equilibrium in this work.

The Langmuir isotherm model assumes monolayer adsorption of the species on the energetically-homogeneous surface sites of the adsorbent. The Langmuir equation is expressed as:

$$q_e = \frac{q_m K_L C_e}{1 + K_L C_e} \tag{3}$$

where q_e is the equilibrium adsorption capacity obtained from the experiment (mg/g), C_e is the equilibrium concentration of dye in solution (mg/L), q_m is maximum adsorption capacity obtained from the isotherm model (mg/g) and K_L is isotherm constants for Langmuir (L/mg) [25].

Separation factor, R_L, can be also determined from the Langmuir plot using the equation below:

$$R_L = \frac{1}{1 + K_L C_0} \tag{4}$$

where R_L's numerical value indicates the type of adsorption involved: irreversible ($R_L = 0$), favourable ($0 < R_L < 1$), linear ($R_L = 1$) or unfavourable ($R_L > 1$). K_L is the Langmuir constant and C_0 is the initial MB dye concentration (ppm) [26].

The Freundlich adsorption isotherm model assumes an energetically heterogeneous adsorption surface. The Freundlich adsorption isotherm equation is as follows:

$$\text{Ln}\, q_e = \ln K_f + \frac{1}{n}\ln C_e \quad (5)$$

where q_e is the amount of adsorbate adsorbed at equilibrium (mg/g) and C_e is the equilibrium concentration of the MB. K_f is the Freundlich constant [(mg/g)(L/mg)$^{1/n}$] and n is adsorption intensity (a dimensionless quantity) known as the heterogeneity factor [27]. The values of K_f and n are calculated from the intercept and the slope on the linear plot of lnq_e vs. lnC_e, respectively. The adsorption process type is determined from the parameter n: the process is linear when $n = 1$, chemical when $n > 1$, and physical when $n < 1$ [28].

The adsorption equilibrium (q_e) vs. the equilibrium concentration (C_e) for the adsorption of MB onto waste wood at 295 k has been presented in Fig. 10. Increasing the initial concentration from 0.15 to 0.75 mg/L shows an increase in the adsorption uptakes from 1.20 to 4.96 mg/g. The greater adsorption uptake at higher initial concentration can be linked to the higher concentration gradient that served as a major driving force to support the adsorption process. A drop in adsorption uptake was observed beyond the initial concentration of 0.68 mg/L which can be linked to the saturation of adsorbent's surface (due to the saturation of the adsorption sites with the MB dye molecules).

The experimental results were fitted to the Langmuir and Freundlich models as shown in Figs. 11 and 12, respectively.

The best fit is determined from the calculated regression coefficient, R^2. The equilibrium isotherm studies show that the MB adsorption on waste wood is best represented by the Freundlich isotherm model (Table 2).

The results obtained in this study were relatively comparable with similar studies in this field. Raw peach shell particles were used to remove MB (at a pH of 5.5 and 295 K). The data were fitted to Langmuir and Freundlich isotherm models, revealing R^2 values of 0.9830 and 0.9966, respectively [29]. Using modified steel slag (at pH = 7 and 293 K), R^2 values of 0.9943 and 0.9340 were obtained for Langmuir and Freundlich isotherms model, respectively [30]. Aqueous medium with lower pH levels (i.e. ~2) was found to adversely impact the removal efficiency. This was linked to the neutralization of free OH groups on the surface of the adsorbent by bonding with H^+ from the acids used for pH adjustment. It was found that at a pH of 5, particles are adequately negatively charged to electrostatically attract the positively charged MB cations. Moreover, the calculated separation factor, R_L, for the Langmuir isotherm was calculated to be 0.256, 0.186, and 0.147 at initial dye concentrations of 10, 15, and 20 ppm, respectively, indicating favorable adsorption ($0 < R_L < 1$).

A comparison of the maximum monolayer adsorption capacity of MB onto various bio-sorbents is presented in Table 3. Considering the preparation and the removal cost and efficiency, waste wood showed to have great potential in practical applications.

3.6. Adsorption kinetics

The dominant controlling mechanisms of the adsorption process, that is, chemical reaction and/or diffusion mass transfer affect the nature and behavior of the kinetics models. The kinetics of the adsorption determines the most suitable operating conditions for a viable full-scale batch process. The study of the adsorption kinetics reveals the solute uptake rate by the adsorbent which dictates the residence time needed in the design of an industrial-scale adsorption unit. The kinetics of MB adsorption by waste wood in this study is analyzed using pseudo-first- and second-order kinetic models (Figs. 13 and 14, respectively).

The pseudo-first-order model describes the adsorption rate based on the adsorption capacity:

$$\text{Log}\left(q_e - q_t\right) = \text{Log}q_e - \frac{K_1}{2.303}t \quad (6)$$

where q_t and q_e (mg/g) are the adsorption capacity at time t and at equilibrium, respectively, K_1 is the rate constant of the pseudo-first-order adsorption (min^{-1}) and t is the contact

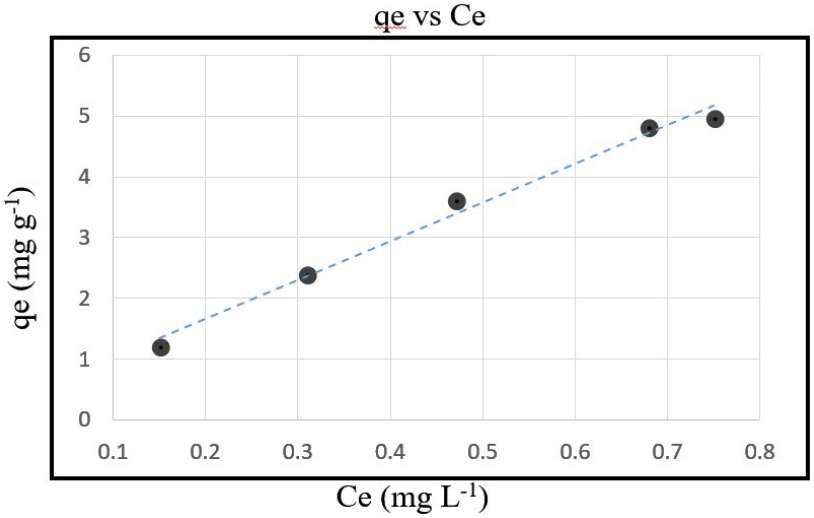

Fig. 10. Adsorption equilibrium (q_e) vs. equilibrium concentration (C_e) for the adsorption of MB onto waste wood at 295 K.

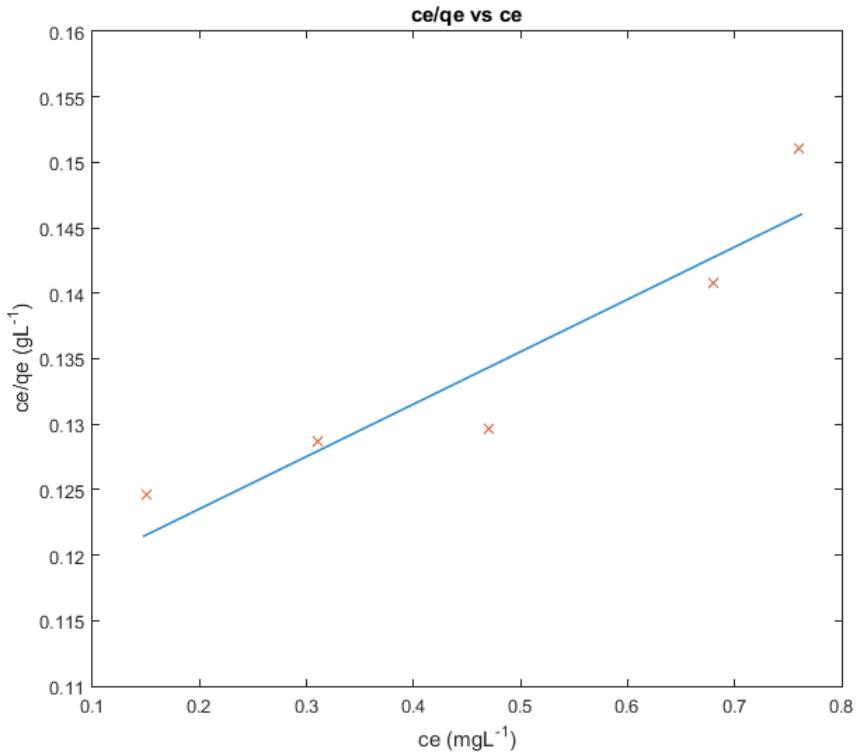

Fig. 11. Langmuir isotherm model for MB adsorption on waste wood at 295 K.

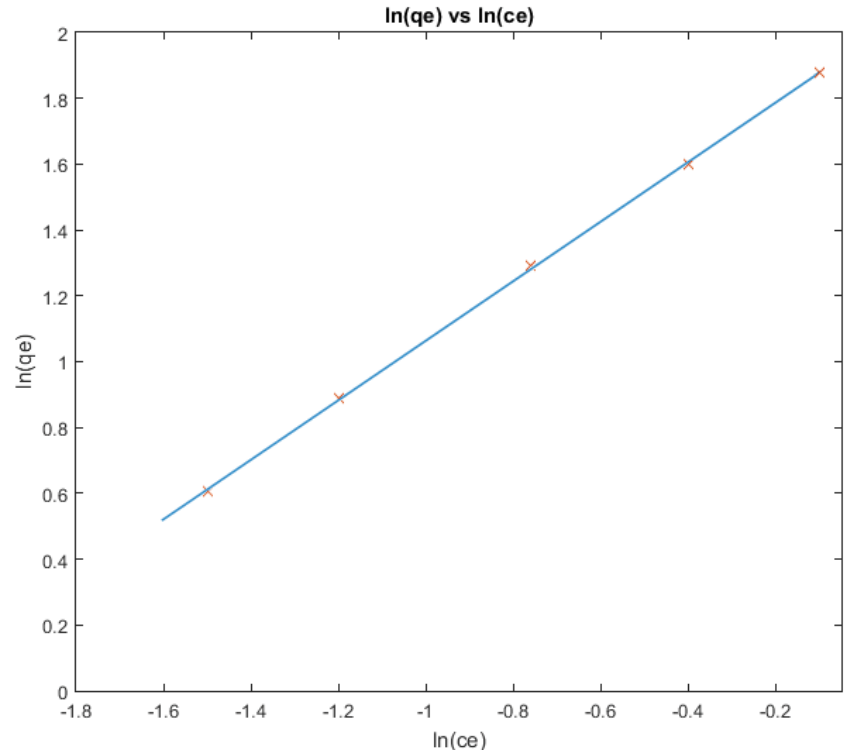

Fig. 12. Freundlich isotherm model for MB adsorption at 295 K.

time (min). Here K_1 and q_e can be determined from the slope and the intercept of the plot of $\log(q_e - q_t)$ vs. t [43]. The kinetics data were also analyzed using the pseudo-second-order model:

$$\frac{t}{q_t} = \frac{1}{k_2 q_e^2} + \frac{1}{q_e} t \tag{7}$$

where k_2 (g/(mg min)) is the rate constant of the second-order adsorption model. The plot of t/q_t vs. t shows a linear relationship that highlights the influence of time on the adsorption capacity. Values of k_2 and the equilibrium adsorption capacity, q_e, are calculated from the intercept and the slope of the plot t/q_t vs. t, respectively.

From Table 4 and Figs. 13 and 14, it is understood that the pseudo-second-order kinetics model can best describe the adsorption of MB on waste wood used in this work. In addition, the pseudo-second-order model shows a higher adsorption capacity compared to the first-order kinetics model as shown in Table 4. Noticeably, a pseudo-second-order kinetics model has been found to be more suitable for data presentation of MB removal using coconut husk [44], sugar beet pulp [23], rejected tea [45] and apricot stones [46]. Due to the good fitting of the second-order kinetic for the entire adsorption period, the adsorption is believed to be controlled via chemisorption.

4. Conclusion

This study investigated the feasibility of using commercially-available waste wood as a low-cost adsorbent to remediate dye-contaminated water. The Taguchi DoE was employed to optimize the experimental parameters affecting MB adsorption using the commercial waste wood, considering the simultaneous interactions among all the investigated operational variables (i.e. pH, MB concentration, adsorbent dosage and mixing speed). Each variable was investigated at four different levels. We employed an orthogonal array with an L16 (4^4) layout to design the experiments. It was found that Taguchi provides a simple, systematic, and efficient method in the optimization of the adsorption experiment. The analyses of the Taguchi DoE revealed that the optimum adsorption conditions were: pH = 5, adsorbent dosage = 4 g/L, initial dye concentration = 0.015 g/L and RPM = 30. The adsorption process was found to be exothermic. Kinetic experiments revealed that adsorption of MB was initially very fast, followed by a slower phase where equilibrium was eventually achieved. A considerable 94% MB removal was observed in the first 5 min of the experiment with an average of around 96% removal at equilibrium. Equilibrium data were best described by the Freundlich isotherm model. The maximum monolayer (theoretical) adsorption capacity was found to be 29.5 mg/g at 295 K. The kinetic studies showed that the MB dye adsorption process followed a pseudo-second-order kinetic model and that the adsorption was controlled by the chemisorption process. Overall, the removal percentage of MB using this specific waste wood biomass was found to be 96%.

Table 2
Isotherm model parameters for the removal of MB by waste wood at 295 K

Isotherm model	Isotherm parameters		
Langmuir	q_m (mg/g)	K_a	R^2
295 K	29.5	0.291	0.8694
Freundlich	K_f [(mg/g)(L/mg)$^{1/n}$]	n	R^2
295 K	90.95	1.13	0.9998

Table 3
Comparison of maximum adsorption capacity values using various bio-sorbents

Adsorbent	q_m (mg/g)	Reference
Marine seaweed	5.23	[31]
Rice husk	9.83	[32]
Brown algae	14.97	[33]
Coconut coir	15.59	[34]
Banana peel	20.8	[35]
Wheat shells	21.50	[36]
Magnetic biochar	22.88	[24]
Activated carbon	24	[37]
Rice hull	29.15	[38]
Lemon peel	29.0	[39]
Waste wood	29.5	In this study
Carbon nanotube	45.66	[40]
Peanut husk	72.13	[41]
Garlic peel	82.64	[42]

Table 4
Experimental adsorption capacity and kinetics parameters of MB adsorption by waste wood using the pseudo-first- and second-order models

	Experimental	Pseudo-first-order			Pseudo-second-order		
Initial dye (g/L)	q_e	q_e	K_1	R^2	q_e	K_2	R^2
0.005	1.20	0.0233	0.0120	0.5866	1.215	2.82	1
0.010	2.40	0.0194	0.0108	0.3958	2.434	4.00	1
0.015	3.61	0.0415	0.0187	0.6847	3.644	1.42	1
0.020	4.82	0.1292	0.0124	0.7890	4.83	0.53	1

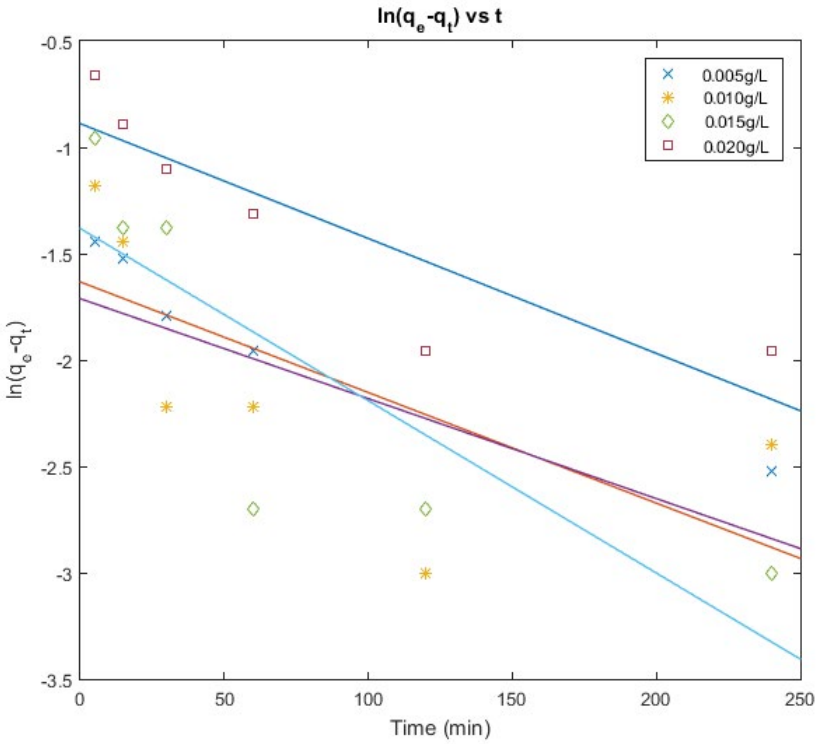

Fig. 13. Pseudo-first-order kinetics for the adsorption of MB by waste wood at 295 K.

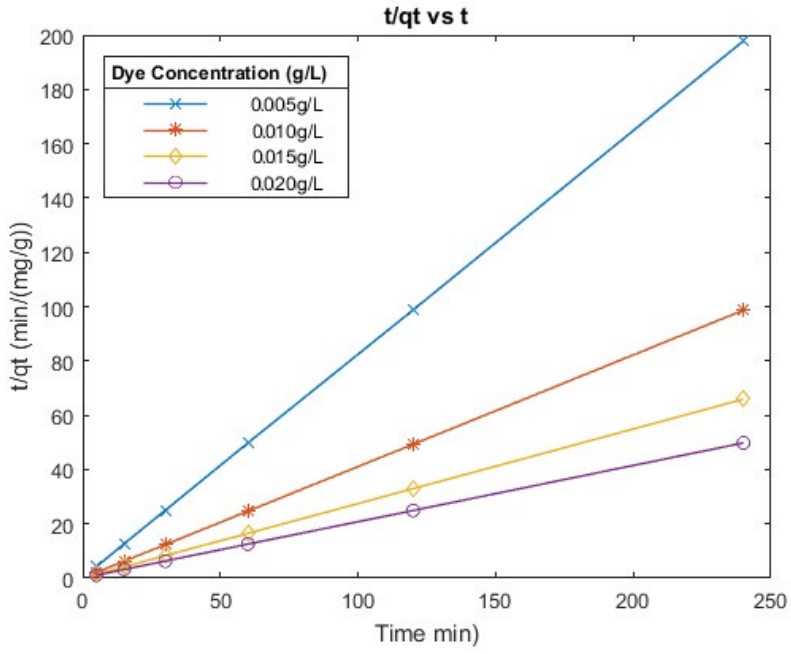

Fig. 14. Pseudo-second-order kinetics for the adsorption of MB by waste wood at 295 K.

Acknowledgment

The authors would like to acknowledge the Advanced Bioprocessing Centre at Brunel University London and Professor Paul Fennell's lab at the Department of Chemical Engineering at Imperial College London for providing us with the facilities, materials, and equipment to conduct this research.

References

[1] R.V. Khandare, S.P. Govindwar, Phytoremediation of textile dyes and effluents: current scenario and future prospects, Biotechnol. Adv., 33 (2015) 1697–1714.

[2] B.J. Wang, Z.S. Bai, H.R. Jiang, P.J. Prinsen, R. Luque, S.L. Zhao, J. Xuan, Selective heavy metal removal and water purification by microfluidically-generated chitosan microspheres: characteristics, modeling and application, J. Hazard. Mater., 364 (2019) 192–205.

[3] M. Shahadat, S.F. Azha, S. Ismail, Z.A. Shaikh, S.A. Wazed, Chapter 16 – Treatment of Industrial Dyes using Chitosan-Supported Nanocomposite Adsorbents, Shahid-ul-Islam, B.S. Butola, Eds., The Impact and Prospects of Green Chemistry for Textile Technology, Elsevier, 2019, pp. 509–539.

[4] F. Charles, S.J. Salami, D.A. Dashak, Teratogenicity, mutagenicity, carcinogenicity, genotoxicity and toxicity of petroleum-contaminated wastewater in Niger-Delta Nigeria, Asian J. Appl. Chem. Res., 4 (2019) 1–9.

[5] M. Kaykhaii, M. Sasani, S. Marghzari, Removal of dyes from the environment by adsorption process, Chem. Mater. Eng., 6 (2018) 31–35.

[6] A. Paz, J. Carballo, M.J. Pérez, J.M. Domínguez, Biological treatment of model dyes and textile wastewaters, Chemosphere, 181 (2017) 168–177.

[7] A. Otondo, B. Kokabian, S. Stuart-Dahl, V.G. Gude, Energetic evaluation of wastewater treatment using microalgae, *Chlorella vulgaris*, J. Environ. Chem. Eng., 6 (2018) 3213–3222.

[8] F. Gündüz, B. Bayrak, Biosorption of malachite green from an aqueous solution using pomegranate peel: equilibrium modelling, kinetic and thermodynamic studies, J. Mol. Liq., 243 (2017) 790–798.

[9] Y. Zhou, L. Zhang, Z.J. Cheng, Removal of organic pollutants from aqueous solution using agricultural wastes: a review, J. Mol. Liq., 212 (2015) 739–762.

[10] Q.M. Liu, Y.Y. Li, H.F. Chen, J. Lu, G.S. Yu, M. Möslang, Y.B. Zhou, Superior adsorption capacity of functionalised straw adsorbent for dyes and heavy-metal ions, J. Hazard. Mater., 382 (2020) 121040.

[11] É. Fenyvesi, K. Barkács, K. Gruiz, E. Varga, I. Kenyeres, G. Záray, L. Szente, Removal of hazardous micropollutants from treated wastewater using cyclodextrin bead polymer – a pilot demonstration case, J. Hazard. Mater., 383 (2020) 121181.

[12] S.M. Soltani, S.K. Yazdi, S. Hosseini, Effects of pyrolysis conditions on the porous structure construction of mesoporous charred carbon from used cigarette filters, Appl. Nanosci., 4 (2014) 551–569.

[13] S.V. Kumar, K.V. Pai, R. Narayanaswamy, M. Sripathy, Experimental optimization for cu removal from aqueous solution using neem leaves based on Taguchi method, Int. J. Sci. Environ. Technol., 2 (2013) 103–114.

[14] X.Y. Chen, D.Q. Chu, L.M. Wang, One-step and green synthesis of novel hierarchical hydrangea flower-like CuO nanostructures with enhanced photocatalytic activity, Physica E, 106 (2019) 194–199.

[15] S. Rana, K. Kumar, Study of phytotoxic effect of textile wastewater on seed germination and seedling growth of *Triticum aestivum*, Int. J. Biosci., 10 (2017) 58.

[16] A. Gürses, Ç. Doğar, M. Yalçın, M. Açıkyıldız, R. Bayrak, S. Karaca, The adsorption kinetics of the cationic dye, methylene blue, onto clay, J. Hazard. Mater., 131 (2006) 217–228.

[17] C.-H. Weng, Y.-T. Lin, T.-W. Tzeng, Removal of methylene blue from aqueous solution by adsorption onto pineapple leaf powder, J. Hazard. Mater., 170 (2009) 417–424.

[18] A. Gürses, S. Karaca, Ç. Doğar, R. Bayrak, M. Açıkyıldız, M. Yalçın, Determination of adsorptive properties of clay/water system: methylene blue sorption, J. Colloid Interface Sci., 269 (2004) 310–314.

[19] S.D. Khattri, M.K. Singh, Colour removal from dye wastewater using sugar cane dust as an adsorbent, Adsorpt. Sci. Technol., 17 (1999) 269–282.

[20] P.S. Kumar, S. Ramalingam, K. Sathishkumar, Removal of methylene blue dye from aqueous solution by activated carbon prepared from cashew nut shell as a new low-cost adsorbent, Korean J. Chem. Eng., 28 (2011) 149–155.

[21] P. Saueprasearsit, M. Nuanjaraen, M. Chinlapa, Biosorption of lead (Pb^{2+}) by *Luffa cylindrical* fiber, Environ. Res., 4 (2010) 157–166.

[22] C. Djilani, R. Zaghdoudi, F. Djazi, B. Bouchekima, A. Lallam, A. Modarressi, M. Rogalski, Adsorption of dyes on activated carbon prepared from apricot stones and commercial activated carbon, J. Taiwan Inst. Chem. Eng., 53 (2015) 112–121.

[23] M.R. Malekbala, S. Hosseini, S.K. Yazdi, S.M. Soltani, M.R. Malekbala, The study of the potential capability of sugar beet pulp on the removal efficiency of two cationic dyes, Chem. Eng. Res. Des., 90 (2012) 704–712.

[24] M. Ruthiraan, E.C. Abdullah, N.M. Mubarak, S. Nizamuddin, Adsorptive removal of methylene blue using magnetic biochar derived from agricultural waste biomass: equilibrium, isotherm, kinetic study, Int. J. Nanosci., 17 (2018) 1850002.

[25] I. Langmuir, The adsorption of gases on plane surfaces of glass, mica and platinum, J. Am. Chem. Soc., 40 (1918) 1361–1403.

[26] I.D. Mall, V.C. Srivastava, G.V.A. Kumar, I.M. Mishra, Characterization and utilization of mesoporous fertilizer plant waste carbon for adsorptive removal of dyes from aqueous solution, Colloids Surf., A, 278 (2006) 175–187.

[27] M. Kamranifar, M. Khodadadi, V. Samiei, B. Dehdashti, M.N. Sepehr, L. Rafati, N. Nasseh, Comparison the removal of reactive red 195 dye using powder and ash of barberry stem as a low cost adsorbent from aqueous solutions: isotherm and kinetic study, J. Mol. Liq., 255 (2018) 572–577.

[28] M. Ghasemi, S. Mashhadi, M. Asif, I. Tyagi, S. Agarwal, V.K. Gupta, Microwave-assisted synthesis of tetraethylene-pentamine functionalized activated carbon with high adsorption capacity for Malachite green dye, J. Mol. Liq., 213 (2016) 317–325.

[29] S. Marković, A. Stanković, Z. Lopičić, S. Lazarević, M. Stojanović, D. Uskoković, Application of raw peach shell particles for removal of methylene blue, J. Environ. Chem. Eng., 3 (2015) 716–724.

[30] M. Cheng, G.M. Zeng, D.L. Huang, C. Lai, Y. Liu, C. Zhang, R. Wang, L. Qin, W.J. Xue, B. Song, S.J. Ye, H. Yi, High adsorption of methylene blue by salicylic acid–methanol modified steel converter slag and evaluation of its mechanism, J. Colloid Interface Sci., 515 (2018) 232–239.

[31] S. Cengiz, L. Cavas, Removal of methylene blue by invasive marine seaweed: caulerpa racemosa var. cylindracea, Bioresour. Technol., 99 (2008) 2357–2363.

[32] Y.C. Sharma, Uma, Optimization of parameters for adsorption of methylene blue on a low-cost activated carbon, J. Chem. Eng. Data, 55 (2009) 435–439.

[33] Y. Ozudogru, M. Merdivan, T. Goksan, Removal of methylene blue from aqueous solutions by brown alga *Cystoseira barbata*, Desal. Water Treat., 62 (2017) 267–272.

[34] Y.C. Sharma, Uma, S.N. Upadhyay, Removal of a cationic dye from wastewaters by adsorption on activated carbon developed from coconut coir, Energy Fuels, 23 (2009) 2983–2988.

[35] G. Annadurai, R.-S. Juang, D.-J. Lee, Use of cellulose-based wastes for adsorption of dyes from aqueous solutions, J. Hazard. Mater., 92 (2002) 263–274.

[36] Y. Bulut, H. Aydın, A kinetics and thermodynamics study of methylene blue adsorption on wheat shells, Desalination, 194 (2006) 259–267.

[37] Y.-S. Ho, R. Malarvizhi, N. Sulochana, Equilibrium isotherm studies of methylene blue adsorption onto activated carbon prepared from *Delonix regia* pods, J. Environ. Prot. Sci., 3 (2009) 111–116.

[38] S.-M. Lee, S.-T. Ong, Oxalic acid modified rice hull as a sorbent for methylene blue removal, APCBEE Procedia, 9 (2014) 165–169.

[39] K.V. Kumar, K. Porkodi, Relation between some two- and three-parameter isotherm models for the sorption of methylene blue onto lemon peel, J. Hazard. Mater., 138 (2006) 633–635.

[40] G.K. Gill, N.M. Mubarak, S. Nizamuddin, H.S. Al-Salim, J.N. Sahu, Column performance of carbon nanotube packed bed for methylene blue and orange red dye removal from waste water, IOP Conf. Ser.: Mater. Sci. Eng., 206 (2017) 012081.

[41] J.Y. Song, W.H. Zou, Y.Y. Bian, F.Y. Su, R.P. Han, Adsorption characteristics of methylene blue by peanut husk in batch and column modes, Desalination, 265 (2011) 119–125.
[42] B.H. Hameed, A.A. Ahmad, Batch adsorption of methylene blue from aqueous solution by garlic peel, an agricultural waste biomass, J. Hazard. Mater., 164 (2009) 870–875.
[43] A.N. Ökte, Adsorption, Kinetics and Photoactivity of ZnO-Supported Fly Ash-Sepiolite Ternary Catalyst, M.A. Farrukh, Ed., Advanced Chemical Kinetics, IntechOpen, 2018, doi: 10.5772/intechopen.70504.
[44] S.R. Dave, V.A. Dave, D.R. Tipre, Coconut husk as a biosorbent for methylene blue removal and its kinetics study, Adv. Environ. Res., 1 (2012) 223–236.
[45] N. Nasuha, B.H. Hameed, Adsorption of methylene blue from aqueous solution onto NaOH-modified rejected tea, Chem. Eng. J., 166 (2011) 783–786.
[46] O.O. Namal, E. Kalipci, Adsorption kinetics of methylene blue using alkali and microwave-modified apricot stones, Sep. Sci. Technol., 54 (2019) 1722–1738.